Journal of Biomolecular NMR, 7 (1996) 107–120
ESCOM

J-Bio NMR 332

^{1}H, ^{15}N and ^{13}C resonance assignments and secondary structure of group II phospholipase A2 from *Agkistrodon piscivorus piscivorus*: Presence of an amino-terminal helix in solution

Roman Jerala*, Paulo F.F. Almeida, Qiang Ye, Rodney L. Biltonen and Gordon S. Rule**

Departments of Biochemistry and Pharmacology, University of Virginia School of Medicine, P.O. Box 440, Charlottesville, VA 22908, U.S.A.

Received 11 September 1995
Accepted 4 January 1996

Keywords: Phospholipase; Secondary structure; Enzyme mechanism

Summary

^{1}H, ^{15}N and ^{13}C resonance assignments are presented for the group II phospholipase A2 (PLA2) from *Agkistrodon piscivorus piscivorus*. The secondary structure of the enzyme has been inferred from an analysis of coupling constants, interproton distances, chemical shifts, and kinetics of amide exchange. Overall, the secondary structure of this PLA2 is similar to the crystal structure of the homologous group II human nonpancreatic secretory phospholipase [Scott, D.L., White, S.P., Browning, J.L., Rosa, J.J., Gelb, M.H. and Sigler, P.B. (1991) *Science*, **254**, 1007–1010]. In the group I enzyme from porcine pancreas, the amino-terminal helix becomes fully ordered in the ternary complex of enzyme, lipid micelles and inhibitor. The formation of this helix is thought to be important for the increase in activity of phospholipases on aggregated substrates [Van den Berg, B., Tessari, M., Boelens, R., Dijkman, R., De Haas, G.H., Kaptein, R. and Verheij, H.M. (1995) *Nature Struct. Biol.*, **2**, 402–406]. However, the group II enzyme from *Agkistrodon piscivorus piscivorus* possesses a defined and well-positioned amino-terminal helix in the absence of substrate. Therefore, there is a clear difference between the conformations of group I and group II enzymes in solution. These conformational differences suggest that formation of the amino-terminal helix is a necessary, but not sufficient, step in interfacial activation of phospholipases.

Introduction

Phospholipases A2 (PLA2, E.C. 3.1.1.4) are calcium-dependent enzymes that specifically hydrolyse the sn-2 ester bond of sn-3 phosphoglycerides (for a review, see Slotboom et al., 1982). The small-molecular-weight (14 kDa) PLA2 are classified in three groups, based on sequence and structure homology (Heinrikson et al., 1977; Scott and Sigler, 1994). Class I PLA2s are present in large concentrations in mammalian pancreas juices and snake venoms of Elapidae and Hydrophidae. Class II PLA2s have been found in a variety of mammalian cells, such as platelets or vascular endothelium cells and also in the arthritic synovial joints. They are thought to play an important physiological role in releasing arachidonic acid, which is a precursor in the formation of inflammatory mediators such as prostaglandins and tromboxanes (Dennis, 1987; Burgoyne and Morgan, 1990). The richest source of group II enzymes have been Crotalidae and Viperidae snake venoms. Group III phospholipases have been found in the venoms of the honeybee and several lizards.

Crystallographic studies of several group I and group II phospholipases have shown that they are structurally quite similar (reviewed by Scott and Sigler, 1994). The main secondary structural features are an α-helix on the amino terminus, two longer parallel α-helices and a two-stranded antiparallel β-sheet. The largest differences between the group I and group II PLA2s are the following (Renetseder et al., 1985; Scott and Sigler, 1994): a seven-residue extension of the carboxy terminus of group II

*On leave from the Department of Biochemistry and Molecular Biology, Jozef Stefan Institute, Jamova 39, Ljubljana, Slovenia.
**To whom correspondence should be addressed.
Abbreviations: PLA2, phospholipase A2; App-D49, phospholipase from *Agkistrodon piscivorus piscivorus*; NOE, nuclear Overhauser effect.

PLA2, insertion of three residues (residues 54–56, the 'elapid loop') in group I PLA2, and one disulfide connecting the carboxyl terminus in group II enzymes instead of linking the amino-terminal helix to the β-sheet (Cys^{11}-Cys^{77}) in group I enzymes.

Phospholipases A2 are remarkable for their ability to hydrolyse aggregated substrate (e.g. micelles or membranes) several orders of magnitude faster than soluble monomeric phospholipids (Slotboom et al., 1982). This 'interfacial activation' is a property of group I and II phospholipases and appears to require an unmodified amino terminus (Van Dam-Mieras et al., 1975; Verheij et al., 1981). The kinetics of hydrolysis of phospholipid vesicles by PLA2 is very complex, with several distinct stages that reflect a complex interaction between the protein and the membrane. It is well established that the activity of PLA2 can be modulated by the physical state of the membrane and depends on properties such as intrinsic membrane curvature (Lichtenberg et al., 1986; Menashe et al., 1986), or the phase separation of immisible components, such as reaction products above the critical mole fraction (Burack et al., 1993). Studies with fluorescence and NMR techniques have indicated the existence of at least three spectroscopically different states of the PLA2 interacting with the membrane (Bell and Biltonen, 1992; Peters et al., 1992; Jain and Maliwal, 1993). These different states could be caused by different modes of interaction of the enzyme as a rigid body with the membrane and/or by lipid-induced conformational changes of the enzyme on the membrane surface.

Structure determination of the complex of several phospholipases with a transition-state analogue inhibitor has led to the proposition that interfacial activation is due to the facilitated transfer of the phospholipid molecule from the membrane to the reactive site through a channel formed by hydrophobic residues (Scott et al., 1990). On the basis of this work, it was suggested that the mechanism of catalysis is identical for group I and II phospholipases A2, although some differences have been observed in the hydrophobic channel, affecting the substrate binding (Scott et al., 1991). This view of interfacial activation did not consider conformational changes of the enzyme, because the crystal structures of the free enzyme and the enzyme bound to an inhibitor were essentially identical. Furthermore, the tertiary structure of phospholipases is thought to be quite rigid, due to the presence of six to seven disulfide bonds.

Recent NMR experiments on the group I PLA2 from porcine pancreas have shown that the solution structure of the protein differs from the crystal structure, thus suggesting an alternative mechanism for interfacial activation (Van den Berg et al., 1995a,b). Van den Berg et al. (1995a) have observed a number of changes in the structure of the enzyme that occur as a result of formation of a complex between protein, lipid, and a transition-state analog. A particularly striking difference between the free and the lipid-bound enzyme is the structure of the amino-terminal helix. In solution, the first three residues of this helix are disordered and the amino terminus is fully accessible to solvent. These residues become partially ordered and begin to demonstrate interactions with the body of the protein when the enzyme is bound to micelles. Upon formation of the ternary complex between the enzyme, micelle, and inhibitor, the amino-terminal residues assume an α-helical conformation. This conformation facilitates the interaction of the amino terminus with a hydrogen-bonding network that is thought to be important for catalysis. Overall, the structure of the protein–lipid–inhibitor complex is similar to the crystal structure, supporting the hypothesis that the crystal structure is the active form of the enzyme.

Recent studies on group II PLA2s have focused on the effect of the lipid substrate on the activation of the enzyme on membrane surfaces (Cho et al., 1988; Biltonen et al., 1991; Bell and Biltonen, 1992; Lathrop and Biltonen, 1992; Burack et al., 1993). Relatively little attention has been paid to structural changes in the protein that may occur during activation. A number of studies have utilized the readily available group II PLA2 from *Agkistrodon piscivorus piscivorus* (App-D49). Fluorescence studies on App-D49 indicate that there are changes in the environment of the tryptophan residues during activation of the enzyme on vesicle surfaces (Bell and Biltonen, 1989). These studies suggest that conformational changes of this enzyme may also play an important role in its activation. Therefore, a key step in understanding the activation of group II enzymes is to investigate the structure of these lipases in solution and on the micellar surface. Although several crystal structures of group II phospholipases have been published, there are no reports of the structures of these enzymes in a noncrystalline environment.

As an initial step in the development of an understanding of the relationship between structure and function of group II PLA2s, we have investigated the properties of App-D49 in solution. In this paper we report the ^{1}H, ^{13}C, and ^{15}N resonance assignments for the enzyme in solution. In addition, we show that the amino-terminal helix of this enzyme is more ordered than in the group I PLA2s. This suggests that changes in the conformation of the amino-terminal helix may play a less significant role in interfacial activation of phospholipases.

Materials and Methods

Sample preparation

Cloning and expression of App-D49 PLA2 have been described by Lathrop et al. (1992). The coding sequence of this gene was modified to incorporate errors in the published protein sequence (see Maragonore and Heinrikson, 1993). The protein sequence has been altered from

TABLE 1
NMR EXPERIMENTS PERFORMED ON App-D49

Experiment	Acquired data matrix size (nucleus)			Spectral widths (Hz)			Number of transients
	t_1	t_2	t_3	ω_1	ω_2	ω_3	
^{15}N HSQC[a]	128 (N)	1024 (H)		1600	4000		8–32
3D TOCSY-HMQC[b] (τ_m = 75 ms)	128 (H)	32 (N)	512 (H)	6500	1600	4000	8
3D NOESY-HMQC[c] (τ_m = 120 ms)	128 (H)	32 (N)	512 (H)	6500	1600	4000	8
3D ^{15}N-^{15}N NOESY[d] (τ_m = 120 ms)	64 (N)	32 (N)	1024 (H)	1600	1600	4000	32
HNCA[e]	32 (N)	48 (C)	576 (H)	1600	3500	4000	32
HN(CO)CA[e]	32 (N)	48 (C)	1024 (H)	1600	3500	4000	32
HNCACB[f]	32 (N)	48 (C)	1024 (H)	3000	1600	4000	32
CBCA(CO)NH[g]	48 (C)	32 (N)	1024 (H)	8400	1600	4000	32
HBHA(CBCACO)NH[h]	48 (H)	32 (N)	1024 (H)	3000	1600	4000	32
HBHA(CBCA)NH[i]	48 (H)	32 (N)	1024 (H)	4000	1600	4000	32
HN(CA)HA[j]	32 (N)	48 (H)	1024 (H)	1600	3000	4000	32
HNCO[e]	32 (C)	48 (CO)	512 (H)	2500	1600	4000	8
HCACO[k]	24 (C)	48 (CO)	512 (H)	3500	2500	2200	16
^{13}C HCCH-TOCSY[l] (τ_m = 19, 28 ms)	128 (H)	36 (C)	512 (H)	3400	3125	3400	8
3D TS (^{1}H, ^{15}N, ^{13}C) HSQC-NOESY-HSQC[m] (τ_m = 120 ms)	32 (N)	48 (C)	512 (H)	1600	8000	6500	32
HNHA[n]	32 (N)	64 (H)	512 (H)	1600	5500	5500	16
HNHB[o]	32 (N)	64 (H)	512 (H)	1600	5500	5500	16
CB(CGCD)HD and CB(CGCDCE)HE[p]	20 (C)	1024 (H)		2500	4000		1536

[a] Bodenhausen and Ruben, 1980.
[b] Driscoll et al., 1990.
[c] Bax et al., 1990a.
[d] Frenkiel et al., 1990; Ikura et al., 1990.
[e] Grzesiek and Bax, 1992a (constant time version).
[f] Wittekind and Mueller, 1993.
[g] Grzesiek and Bax, 1992b.
[h] Grzesiek and Bax, 1993.
[i] Wang et al., 1994.
[j] Clubb et al., 1992.
[k] Kay et al., 1990.
[l] Bax et al., 1990b.
[m] Jerala and Rule, 1995.
[n] Vuister and Bax, 1993; Bax et al., 1994.
[o] Archer et al., 1991; Bax et al., 1994.
[p] Yamazaki et al., 1993.

the sequence of the native enzyme by replacement of the amino-terminal asparagine residue with serine to achieve proper processing of amino-terminal methionine by *E. coli*. The recombinant PLA2 was characterized by measurement of K_m and V_{max} on a monomeric substrate (dicaprylphosphatidylcholine) as well as measurement of the time course of hydrolysis on dipalmitoylphosphatidylcholine vesicles. These properties were essentially the same as found for the enzyme obtained from venom.

Labeled App-D49 (^{13}C and ^{15}N) was prepared by growing the bacteria in minimal media, supplemented with ^{15}N $(NH_4)_2SO_4$ (1 g/l) or ^{13}C glucose (3 g/l). The isolation and refolding procedure reported previously (Lathrop et al., 1992) has been altered to increase the yield of refolded protein from 25% to 50–70% (Almeida et al., 1995). This new scheme was based on the principle that efficient renaturation of PLA2 will occur if the protein is refolded under conditions such that the native conformation is only marginally more stable than the unfolded one. In this environment, misfolded structures can reach the native state before becoming kinetically trapped in inactive configurations.

Fluorescence spectroscopy was used to determine the thermodynamic stability of App-D49 (data not shown). The intrinsic fluorescence of App-D49 decreased at a guanidine hydrochloride concentration of 3.5–4.0 M. When the experiment was repeated under reducing conditions, a similar decrease in fluorescence was observed at 0.5–1.5 M guanidine hydrochloride concentration. Addition of Ca^{2+} to 10 mM only resulted in a marginal increase of stability, but was nevertheless included in all refolding experiments. Based on these results, refolding experiments were performed at guanidine hydrochloride concentrations between 0.5 and 1.5 M. These experiments indicated that concentrations between 0.8 and 1 M gave the highest yield of active enzyme (data not shown). During the course of these experiments it was also determined that the yield of refolding is very sensitive to pH; the best results were obtained at pH = 7.8–7.9 (data not shown).

Sulfonated PLA2 was purified from inclusion bodies, as described previously (Lathrop et al., 1992). The purified protein was refolded in a mixture adjusted to the following final concentrations: 5 μM App-D49, 0.8 M guanidine hydrochloride, 2.5 mM reduced glutathione (Sigma, St. Louis, MO), 0.5 mM oxidized glutathione (Sigma), 20 mM Tris-HCl, pH 7.85, 1 mM EDTA, and 10 mM $CaCl_2$. Note the reduction in the concentration of App-D49 as well as the omission of the dodecyl-β-D-maltoside in the modified scheme. The extent of refolding was measured by monitoring the enzymatic activity using 0.20 μM App-D49 and 13 mM 1,2-di-butyroyl-*sn*-glycero-3-phosphocholine in 50 mM KCl, 10 mM $CaCl_2$, pH 8.0, at room temperature, and comparing this to the activity of venom App-D49 under the same conditions. Refolding

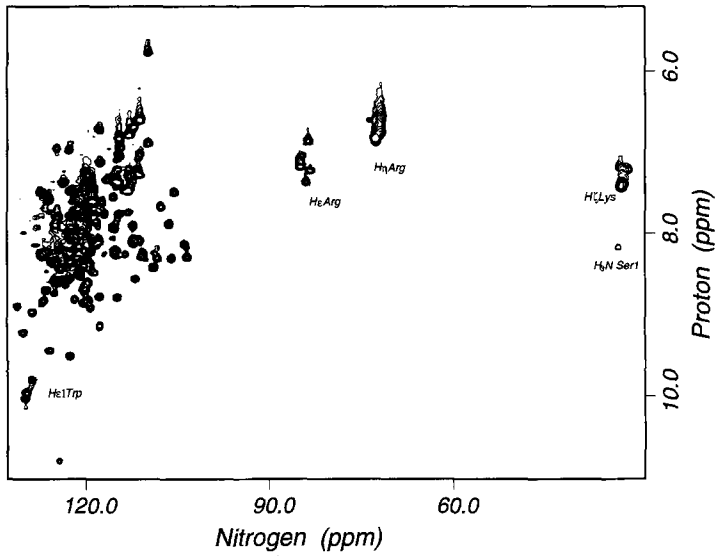

Fig. 1. ^{15}N-^{1}H heteronuclear single-quantum spectrum of App-D49. Cross peaks from the side chains of Trp, Arg and Lys as well as the amino terminus are labeled. All other peaks arise from main-chain amides and the side chains of Asn and Gln.

was allowed to proceed for about 15–20 h (either at 4 or 20 °C), after which the solution was diluted 1:10 into 20 mM Tris, pH 7.8. This solution (0.08 M in guanidine hydrochloride) was then loaded onto an SP-Sepharose (Sigma) ion exchange chromatography column equilibrated with the same buffer, and eluted at 20 ml/h with a 0.0–0.4 M NaCl gradient in the same buffer. Finally, the protein solution was dialyzed extensively against water at 4 °C and lyophilized.

The sample for NMR spectroscopy was prepared by dissolving 7 mg (^{15}N and ^{13}C labeled) or 12 mg (^{15}N labeled) lyophilized protein in 0.45 ml of 20 mM sodium phosphate buffer, pH 4.3, and 100 mM KCl. D_2O was added to 5% for all experiments except for the HCCH-TOCSY experiment and amide exchange experiments, which were done in buffered D_2O. All NMR experiments were performed at 40 °C.

NMR spectroscopy

NMR spectra were recorded on a 500 MHz Varian UnityPlus spectrometer, equipped with a Nalorac 5 mm triple resonance probe with a shielded Z gradient coil. Quadrature detection was achieved with the States-TPPI method (Marion et al., 1989a). Table 1 provides a list of the NMR experiments that were performed, along with basic experimental conditions. Pulsed field gradients were used to suppress the water signal and to remove undesired coherences. Gradients were implemented in the following pulse sequences (see Bax and Pochapsky, 1992): HNCA, HN(CO)CA, HNCACB, CBCA(CO)NH, HBHA(CBCA-CO)NH, HN(CA)HA, HCACO, HCCH-TOCSY and HNHB. Additional suppression of the water signal was accomplished using spin-lock purge pulses (Messerle et al., 1989) and spectral deconvolution in the time domain (Marion et al., 1989b).

A spectral width of 1600 Hz was employed for the ^{15}N dimension in all experiments except in the ^{15}N HSQC, causing folding of some of the side-chain amides. Extensive folding to achieve higher resolution in the carbon dimension was employed only in the HCCH-TOCSY experiment (spectral width of 3400 Hz). Otherwise a spectral width of 8400 Hz was used in the carbon dimension. The ^{1}H and ^{13}C chemical shifts are given relative to 3-(trimethylsilyl)propionic acid. The ^{15}N chemical shifts were indirectly referenced by multiplying the frequency of the standard with the ratio of the zero-point frequencies of ^{15}N with ^{1}H, corrected for the temperature of the solution (Edison et al., 1994).

The kinetics of amide exchange were determined by measuring the intensity of cross peaks in a ^{15}N-HSQC spectrum at various times after a sample of ^{15}N-labeled App-D49 was dissolved in D_2O. The first ^{15}N spectrum was completed 3 h after dissolution in D_2O. Therefore, amides that exchange with a rate greater than approximately 1–2 h^{-1} could not be detected. The intensity of the cross peaks as a function of time was fit to a single exponential function to obtain the rate constant for exchange.

The three-bond coupling constant $J_{H^N-H^\alpha}$ was obtained from an analysis of the HNHA spectrum. The coupling constant is calculated from the fraction of magnetization transferred from the HN to the H^α proton. These coupling constants were related to the ϕ dihedral angle using the relationship described by Vuister and Bax (1993).

Transformations and other manipulation of data, as well as analysis of spectra, was done using the FELIX software (Biosym Technologies, San Diego, CA) on a Silicon Graphics INDIGO workstation. Linear prediction of about 30% additional data points was used in most of the indirect heteronuclear dimensions (Olejniczak and Eaton, 1990). In some cases, the first one or two points

were also linearly predicted to flatten the baseline. Implementation of all the pulse sequences used here, as well as the FELIX processing macros, are available upon request from the authors.

Results

Resonance assignments

Strategy for the backbone assignments

A ^{15}N-^{1}H HSQC spectrum of App-D49 is shown in Fig. 1. Note the presence of several peaks around 40 ppm, which may represent the amino-terminal amide proton and/or side chains of lysine residues. The spectrum in Fig. 1 shows 114 well-resolved peaks of the expected 138 peaks from main-chain amides (117), H^{ε} of tryptophan (3), asparagine and glutamine side chains (18). The lack of cross peaks suggests considerable overlap of nitrogen and amide-proton chemical shifts. Three-dimensional ^{15}N-TOCSY-HMQC and ^{15}N-NOESY-HMQC spectra were used in an attempt to apply conventional proton-based sequential assignments to App-D49 (Billeter et al., 1982; Wüthrich, 1986). Using sequential NOEs between H^{α}-HN, H^{β}-HN and HN-HN, we could only ascertain reliable connectivities for residues 89–95, 50–55 and 102–107. Since this strategy only assigned a small number of the residues, triple resonance techniques were used to complete the assignments.

Triple resonance multidimensional experiments with a uniformly ^{15}N-/^{13}C-labeled sample were performed to establish scalar connectivities (see Table 1). Representative sections of the HNCA and CBCA(CO)NH spectra are shown in Fig. 2. The first step in the assignment procedure was to obtain information on the type of amino acid for each spin system. The HNCACB spectrum in combination with the CBCA(CO)NH spectrum, and the HBHA(CBCA)NH spectrum in combination with the HBHA(CBCACO)NH spectrum provided intraresidue shifts for C^{α}, C^{β}, H^{α} and H^{β} atoms. This information was particularly useful for identification of Gly, Ala, Ser and Thr residues (Grzesiek and Bax, 1993). Glycine residues were also recognized by the absence of intraresidue cross peaks in the HN(CA)HA spectrum. A ^{15}N-TOCSY-HMQC spectrum provided additional information on the type of spin system, although it was often impossible to distinguish glycine from serine residues.

Sequential connectivities were determined by several parallel pathways, using several or all of the C^{α}, C^{β}, H^{α}, H^{β} and CO resonances for each connectivity. The combination of HNCA and HN(CO)CA experiments provides connectivities from one C^{α} to the preceding C^{α}. The HN(CO)CA spectrum identifies the interresidue cross peak and can indicate degeneracies in the chemical shifts of C^{α} resonances from adjacent residues. In parallel, identification of inter- and intraresidue H^{α} chemical shifts were obtained from the HN(CA)HA spectrum in combination with the HNHA and HBHA(CBACO)NH spectra. A combination of the C^{α} and H^{α} chemical shifts leads to the unique assignment of a number of residues (see Fig. 3). However, approximately 50% of the residues showed

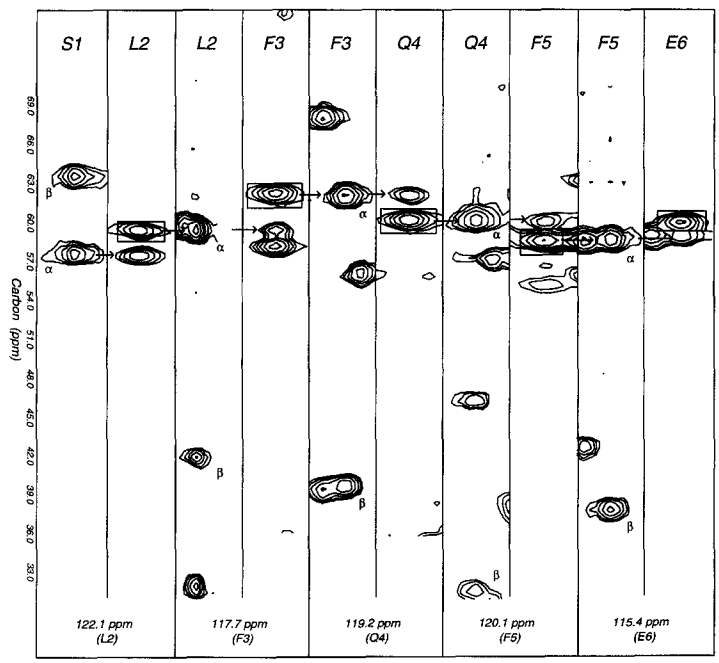

Fig. 2. HNCA and CBCA(CO)NH spectra of App-D49. Slices at the nitrogen frequencies of residues Leu^{2} to Glu^{6} are shown. The left section of each panel is part of the CBCA(CO)NH spectrum and provides the C^{α} and C^{β} shifts of the preceding residue. For example, the region of the CBCA(CO)NH spectrum at the amide frequency of Leu^{2} (122.1 ppm) provides the carbon shifts for Ser^{1}. The right section of each panel is part of the HNCA spectrum. The peaks in boxes are intraresidue correlations. The arrows connect interresidue C^{α} cross peaks.

TABLE 2
^{1}H, ^{15}N AND ^{13}C CHEMICAL SHIFTS FOR App-D49 PLA_2 AT pH 4.3 AND 40 °C

Residue	^{15}N	HN	CO	H^{α}	C^{α}	H^{β}	C^{β}	Other ^{1}H	Other ^{13}C, ^{15}N
Ser[1]	32.3	8.17	172.9	3.81	57.8	3.46	63.7		
Leu[2]	122.1	8.38	178.1	4.51	59.1	1.83	41.7	H^{γ} 1.76; H^{δ} 1.11, 1.27	C^{γ} 41.7; $C^{\delta 1}$ 25.6; $C^{\delta 2}$ 25.1
Phe[3]	117.7	8.14	178.1	4.40	61.1	3.11, 2.95	38.8	H^{δ} 7.78	
Gln[4]	119.2	7.33	177.5	3.89	59.8	2.07, 1.75	31.2	H^{γ} 2.24; H^{ε} 7.05, 6.82	C^{γ} 35.7; N^{ε} 112.1
Phe[5]	120.1	8.29	177.4	4.42	58.8	3.75, 3.41	37.9	H^{δ} 7.20; H^{ε} 7.04	
Glu[6]	115.4	8.18	179.2	3.73	59.6	2.05	28.4	H^{γ} 2.34	C^{γ} 34.7
Lys[7]	120.9	7.50	179.5	3.95	60.0	2.03, 1.76	31.9	H^{γ} 1.31; H^{δ} 1.50; H^{ε} 2.87	C^{γ} 50.6; C^{δ} 29.4; C^{ε} 42.5
Leu[8]	121.7	8.37	179.2	3.74	59.1	1.94, 1.02	41.7	H^{γ} 1.65; H^{δ} 0.50, 0.22	C^{γ} 27.6; $C^{\delta 1}$ 25.6; $C^{\delta 2}$ 22.9
Ile[9]	119.3	8.45	179.9	3.18	67.3	1.54	38.7	H^{γ} 0.13, 0.52; H^{δ} −0.30	C^{γ} 15.7; $C^{\gamma 2}$ 18.1; C^{δ} 39.7
Lys[10]	124.4	7.92	179.6	4.18	59.4	1.84	31.9	H^{γ} 1.33; H^{δ} 1.63; H^{ε} 2.93	C^{γ} 25.2; C^{δ} 29.3; C^{ε} 42.5
Lys[11]	119.7	8.18	178.1	4.03	58.7	1.83	31.9	H^{γ} 1.41; H^{δ} 1.59; H^{ε} 2.84	C^{γ} 25.4; C^{δ} 29.3; C^{ε} 42.5
Met[12]	112.1	7.95	177.7	4.62	56.2	1.98, 1.70	33.6	H^{γ} 2.50, 2.22	C^{γ} 32.6
Thr[13]	105.6	8.35	175.1	4.38	62.9	4.03	73.0	H^{γ} 1.00	C^{γ} 22.0
Gly[14]	110.9	8.10	173.4	3.89, 3.70	46.0				
Lys[15]	121.0	8.28	174.5	4.20	54.2	1.26, 0.96	33.9	H^{γ} 0.52; H^{δ} 0.34; H^{ε} 1.75	C^{γ} 24.2; C^{δ} 28.1; C^{ε} 42.0
Ser[16]	112.0	8.08	176.6	4.29	57.9	3.77	64.3		
Gly[17]	117.6	9.07	176.4	3.84	48.1				
Met[18]	121.2	8.71	177.9	4.21	58.3	2.45, 1.92	32.1	H^{γ} 1.63	C^{γ} 27.8
Leu[19]	118.6	7.47	177.3	4.16	56.9	1.33, 1.02	42.5	H^{γ} 0.90; H^{δ} 0.73, 0.59	C^{γ} 21.4; $C^{\delta 1}$ 24.8; $C^{\delta 2}$ 24.2
Trp[20]	114.7	7.45	177.4	4.35	58.5	2.18	31.3	H^{δ} 7.16; $H^{\varepsilon 1}$ 9.80; $H^{\zeta 2}$ 7.16	N^{ε} 128.9
Tyr[21]	114.9	8.08	174.4	4.76	58.7	2.27	39.7		
Ser[22]	112.5	7.33	173.4	4.29	59.8	3.97	64.8		
Ala[23]	124.7	6.94	174.2	4.35	52.0	0.69	18.0		
Tyr[24]	124.8	7.94	174.5	4.99	57.9	2.74	41.9	H^{δ} 7.00	
Gly[25]	113.3	8.30	172.8	3.46, 2.60	44.8				
Cys[26]	122.3	11.17	176.1	4.76	56.7		33.2		
Tyr[27]	131.2	7.97	181.8	4.14					
Cys[28]			179.4		50.4				
Gly[29]	116.4	7.24	172.8	3.11	45.3				
Trp[30]	120.8	8.02	176.4	4.76	57.5	3.20	29.7	H^{δ} 7.46; $H^{\varepsilon 1}$ 10.04; $H^{\zeta 2}$ 7.22; $H^{\varepsilon 3}$ 7.25	N^{ε} 130.0
Gly[31]	110.7	8.36	174.3	3.67	46.4				
Gly[32]	107.7	7.83	172.7	3.54	46.4				
Gln[33]	117.7	6.76	173.1	4.44	55.3	2.11, 1.82	31.5	H^{γ} 2.01; H^{ε} 7.28, 6.70	C^{γ} 34.8; N^{ε} 112.9
Gly[34]	103.4	8.16	175.7	4.08, 3.86	45.6				
Arg[35]	127.2	8.93	173.2	4.76	53.4	1.55	31.3	H^{γ} 1.44; H^{δ} 3.01	C^{γ} 32.0; C^{δ} 43.7
Pro[36]			178.4	4.60	62.4	1.67	31.0	H^{γ} 1.60, 1.41; H^{δ} 3.02	C^{γ} 31.9; C^{δ} 42.6
Lys[37]	124.3	10.82	175.6	3.88	56.3	1.08, 0.72	32.7	H^{γ} 1.09; H^{δ} 1.57; H^{ε} 2.74	C^{γ} 24.6; C^{δ} 31.5; C^{ε} 42.5
Asp[38]	116.4	7.37	175.8	4.41	52.3	3.08, 2.73	40.9		
Ala[39]	120.8	8.56	179.6	3.98	56.5	1.28	19.1		
Thr[40]	118.3	8.51	175.7	3.72	70.5	4.16	70.4	H^{γ} 0.92	C^{γ} 22.7
Asp[41]	121.8	8.85	179.9	5.28	56.4	2.75	41.8		
Arg[42]	119.6	8.63	178.0	3.87	60.6	2.03, 1.53	29.0	H^{γ} 1.73; H^{δ} 3.14, 2.93	C^{γ} 29.2; C^{δ} 43.0
Cys[43]	119.1	8.48	179.1	4.21	57.4	2.49	37.4		
Cys[44]	120.2	8.06	175.1	4.05	59.5	1.98	44.7		
Phe[45]	125.0	8.56	176.0	3.76	61.6	2.92, 2.12	39.6	H^{δ} 7.10	
Val[46]	119.9	8.74	177.7	2.95	67.1	1.86	31.6	H^{γ} 1.39	C^{γ} 25.4
His[47]	119.8	7.71	175.7	4.30	60.1	2.83	28.1	$H^{\delta 2}$ 6.75; $H^{\varepsilon 1}$ 8.18	
Asp[48]	120.0	8.17	179.4	4.12	56.9	3.00, 2.79	37.9		
Cys[49]	120.4	8.17	176.4	4.14	58.2	2.66	37.5		
Cys[50]	123.1	8.63	178.3	3.94	61.9	3.19	36.9		
Tyr[51]	119.4	8.19	179.4	4.19	58.8	3.14, 2.94	36.5	H^{δ} 6.75	
Gly[52]	106.1	7.94	174.5	3.89	46.8				
Lys[53]	117.5	7.16	176.5	4.27	56.3	1.89, 1.79	33.1	H^{γ} 1.27; H^{δ} 1.48; H^{ε} 2.78	C^{γ} 25.4; C^{δ} 25.6; C^{ε} 42.6
Val[54]	122.5	7.51	175.1	3.85	63.8	2.11	31.5	H^{γ} 0.76, 0.71	$C^{\gamma 1}$ 21.9; $C^{\gamma 2}$ 24.1
Thr[55]	119.1	8.28	175.2	4.59	61.5	4.05	71.0	H^{γ} 1.03	C^{γ} 21.5
Gly[56]	111.7	8.60	173.4	4.02, 3.79	45.7				
Cys[57]	113.5	7.51	170.8	4.74	57.0	3.38, 3.17	36.6		
Asn[58]	119.3	8.99	173.3	5.07	50.6	1.76	40.2	H^{δ} 7.78, 7.07	N^{δ} 115.2
Pro[59]			175.1	3.92	64.4	0.81, 0.40	31.5	H^{γ} 1.46; H^{δ} 4.22	C^{γ} 29.4; C^{δ} 59.9
Lys[60]	111.2	7.27	178.5	4.16	59.3	1.73	33.5	H^{γ} 1.30; H^{δ} 1.62; H^{ε} 2.84	C^{γ} 25.4; C^{δ} 29.6; C^{ε} 42.5
Met[61]	114.2	6.97	176.5	4.63	55.4	2.00, 1.58	35.4	H^{γ} 2.47, 2.28	C^{γ} 32.3
Asp[62]	120.6	8.44	175.9	4.63	56.4	2.53, 1.97	41.0		

TABLE 2
(continued)

Residue	^{15}N	HN	CO	H^{α}	C^{α}	H^{β}	C^{β}	Other ^{1}H	Other ^{13}C, ^{15}N
Ile[63]	124.4	8.63	175.6	3.87	61.4	1.60	39.5	H^{γ} 0.87, 0.79; H^{δ} 0.79	$C^{\gamma 1}$ 24.4; $C^{\gamma 2}$ 18.2; C^{δ} 13.7
Tyr[64]	125.6	8.40	175.9	5.21	54.4	3.44, 2.60	41.4	H^{δ} 6.65	
Thr[65]	117.6	8.80	173.2	4.66	62.5	3.74	71.1	H^{γ} 1.08	C^{γ} 21.8
Tyr[66]	123.9	8.44	172.6	5.49	56.8	3.16, 2.85	41.5	H^{δ} 6.85; H^{ε} 5.57	
Ser[67]	114.9	8.85	172.6	4.55	56.7	3.68	66.4		
Val[68]	122.6	8.59	175.4	4.87	61.9	1.93	32.6	H^{γ} 0.86, 0.63	$C^{\gamma 1}$ 21.8; $C^{\gamma 2}$ 21.6
Glu[69]	126.8	8.74	175.9	4.59	54.9	1.83, 1.74	31.3	H^{γ} 2.09	C^{γ} 34.9
Asn[70]	126.0	9.48	175.0	4.29	54.9	2.91, 2.61	37.8	H^{δ} 7.50, 6.82	N^{δ} 114.0
Gly[71]	103.1	8.32	172.6	4.04, 3.39	45.8				
Asn[72]	118.5	7.82	173.7	4.95	51.7	2.63	41.0	H^{δ} 7.38, 6.85	N^{δ} 115.3
Ile[73]	124.0	8.61	175.1	4.40	61.3	1.50	39.1	H^{γ} 0.95, 0.63; H^{δ} 0.73	$C^{\gamma 1}$ 28.3; $C^{\gamma 2}$ 18.3; C^{δ} 14.8
Val[74]	130.1	9.25	176.4	4.12	61.8	1.90	33.5	H^{γ} 0.71	C^{γ} 21.4
Cys[75]	128.9	9.08	174.6	4.81	56.2	2.97	40.8		
Gly[76]	112.0	8.16	174.0	4.52, 3.61	44.6				
Gly[77]	108.7	8.46	174.1	4.31, 3.96	44.7				
Thr[78]	108.0	8.32	174.2	4.31	62.3	3.78	69.9	H^{γ} 1.05	C^{γ} 22.2
Asn[79]	122.2	8.02	174.3	5.18	51.1	2.82	40.4	H^{δ} 7.95, 7.38	N^{δ} 122.8
Pro[80]			177.9	4.16	65.7		32.2		
Cys[81]	120.2	7.82	176.6	4.23	61.4	2.26, 1.89	40.2		
Lys[82]	118.7	7.84	177.9	3.81	61.5	3.08	33.0		
Lys[83]	118.7	7.64	177.9	4.23	60.4	2.19	33.0		
Gln[84]	119.4	7.63	178.9	3.87	59.6	1.74, 1.60	28.5	H^{ε} 7.93, 7.38	N^{ε} 112.9
Ile[85]	118.5	7.64	177.1	3.09	67.1	1.89	38.5	H^{γ} 0.41, 0.96; H^{δ} 0.69	$C^{\gamma 1}$ 28.1; $C^{\gamma 2}$ 20.7; C^{δ} 16.4
Cys[86]	119.6	7.38	175.7	2.60	60.5	1.99	39.1		
Glu[87]	118.9	8.63	180.9	3.88	59.5	1.89	28.4	H^{γ} 2.26	C^{γ} 32.6
Cys[88]	118.4	8.17	178.4	4.47	56.3	3.30, 2.68	36.4		
Asp[89]	127.1	8.28	176.2	3.87	58.2	2.80, 2.60	39.6		
Arg[90]	122.5	9.57	176.8	3.61	60.1	1.70, 1.44	30.9	H^{γ} 1.22; H^{δ} 2.73	C^{γ} 26.2; C^{δ} 42.1
Ala[91]	118.1	7.90	180.3	3.87	55.2	1.34	18.3		
Ala[92]	119.9	7.29	176.6	4.01	54.9	0.84	19.0		
Ala[93]	119.9	8.11	178.9	3.64	56.2	1.11	17.5		
Ile[94]	116.8	7.81	176.1	3.31	66.0	1.58	38.3	H^{γ} 0.81, 0.74; H^{δ} 0.80	$C^{\gamma 1}$ 24.9; $C^{\gamma 2}$ 17.8; C^{δ} 14.4
Cys[95]	121.4	7.79	179.0	4.17	61.1	3.14, 2.82	35.9		
Phe[96]	120.4	8.90	179.5	4.41	58.4	2.92, 2.77	37.5	H^{δ} 6.57; H^{ε} 7.23	
Arg[97]	120.7	7.67	178.6	3.68	60.2	2.17, 1.53	29.5	H^{γ} 2.17, 1.91; H^{δ} 3.29, 3.13	C^{γ} 18.9; C^{δ} 43.6
Asp[98]	119.7	8.88	176.9	4.41	56.9	2.66	39.8		
Asn[99]	115.3	7.59	173.9	5.06	54.2	2.71, 2.29	40.0	H^{δ} 7.29, 6.64	N^{δ} 115.9
Leu[100]	123.7	7.43	179.5	4.17	58.6	1.78, 1.44	42.8	H^{γ} 1.89; H^{δ} 0.76, 0.62	C^{γ} 27.3; $C^{\delta 1}$ 25.8; $C^{\delta 2}$ 25.0
Lys[101]	114.9	8.26	177.6	4.17	59.1	1.85	32.4	H^{γ} 1.42; H^{δ} 1.64; H^{ε} 2.93	C^{γ} 25.4; C^{δ} 29.6; C^{ε} 42.4
Thr[102]	105.4	7.53	173.7	4.64	61.1	4.63	70.5	H^{γ} 1.15	C^{γ} 22.4
Tyr[103]	127.4	7.52	175.8	4.01	61.3	3.08, 2.89	39.0	H^{δ} 7.04	
Asp[104]	131.4	8.95	174.9	5.07	52.5	3.06, 2.58	41.2		
Ser[105]	119.9	8.67	176.2	4.11	60.7	4.06	63.2		
Lys[106]	122.2	8.09	178.1	4.07	59.6	1.79	32.0	H^{γ} 1.33; H^{δ} 1.61; H^{ε} 2.88	C^{γ} 25.5; C^{δ} 29.3; C^{ε} 42.5
Thr[107]	113.0	7.35	176.3	3.87	65.3	2.79	69.2	H^{γ} 0.18	C^{γ} 21.9
Tyr[108]	114.8	7.40	176.2	4.51	59.3	1.65	37.8	H^{δ} 6.80	
Trp[109]	124.4	8.27	176.1	4.82	59.3	3.54, 3.14	29.3	H^{δ} 7.09; $H^{\varepsilon 1}$ 9.97; $H^{\zeta 2}$ 7.33; $H^{\varepsilon 3}$ 6.43	N^{ε} 129.8
Lys[110]	125.2	8.79	175.1	3.16	58.0	1.41, 1.27	28.8	H^{γ} 0.38, 0.01; H^{δ} 1.05; H^{ε} 2.37, 2.27	C^{γ} 25.3; C^{δ} 29.2; C^{ε} 45.4
Tyr[111]	122.7	7.00	175.8	4.50	56.5	3.09	39.5	H^{δ} 6.46	
Pro[112]			177.1	4.16	63.1	1.95, 1.44	31.7	H^{γ} 1.65; H^{δ} 2.42	C^{γ} 27.9; C^{δ} 35.8
Lys[113]	126.2	8.26	179.2	3.84	59.3	1.51	31.7	H^{γ} 1.30; H^{δ} 1.51; H^{ε} 2.58	C^{γ} 25.8; C^{δ} 32.0; C^{ε} 42.5
Lys[114]	117.7	8.13	176.5	3.92	58.3	2.12, 1.61	31.3	H^{γ} 1.08; H^{δ} 1.44; H^{ε} 2.73	C^{γ} 24.4; C^{δ} 25.5; C^{ε} 42.4
Asn[115]	117.2	7.65	175.7	4.60	53.7	3.03, 2.42	37.9	H^{δ} 5.80, 6.91	N^{δ} 110.9
Cys[116]	122.1	7.81	174.4	4.95	56.2	3.35, 3.08	42.8		
Lys[117]	120.3	7.56	175.7	4.24	56.4	1.75, 1.62	32.6	H^{γ} 1.27; H^{δ} 1.54; H^{ε} 2.85	C^{γ} 25.3; C^{δ} 29.2; C^{ε} 42.5
Glu[118]	120.4	8.02	175.0	4.21	56.6	1.96, 1.79	29.9	H^{γ} 2.09	C^{γ} 36.4
Glu[119]	121.1	8.24	176.4	4.13	57.4	1.84	29.5	H^{γ} 2.23	C^{γ} 35.6
Ser[120]	119.8	8.42	174.3	4.30	59.2	3.83	64.5		
Glu[121]	126.1	7.57	173.1	4.44	54.1	1.63	29.9	H^{γ} 2.03	C^{γ} 35.1
Pro[122]			176.9	4.51	63.1	2.14, 1.89	31.9	H^{γ} 1.90; H^{δ} 3.55, 3.73	C^{γ} 27.4; C^{δ} 51.3
Cys[123]	124.3	8.21	179.9	4.25	57.8	2.87, 2.58	39.2		

degeneracies in assignment. A number of these degeneracies were resolved by obtaining C^{α} and C^{β} chemical shifts from the HNCACB and CBCA(CO)NH spectra. These spectra provided sufficient information to uniquely assign all but 20 of the residues in App-D49 (Fig. 3). By inclusion of the C^{α} and H^{α} chemical shifts, 12 of these degeneracies could be resolved. All sequential connectivities were finally resolved by correlation of the carbonyl chemical shift. The HNCO and HCACO spectra provide connectivities through (HN_i, N_i)-(CO_{i-1}) and (H_i)-(C_i^{α})-(CO_i), thereby having to satisfy five chemical shifts. These additional correlations removed all of the remaining degeneracies in the main-chain assignments (see Fig. 3).

Proline residues were assigned starting from the CO frequency (obtained from the HNCO spectrum), followed by the C^{α} and H^{α} frequencies, which were obtained from the HCACO spectrum. The backbone assignments were confirmed by the presence of sequential NOEs (90 H^{α}-HN, 79 H^{β}-HN and 91 HN-HN NOEs) that were obtained from the ^{15}N-NOESY-HMQC spectrum. An additional 11 HN-HN NOE cross peaks, for residues with degenerate NH shifts, were obtained from the ^{15}N-HN-HN NOESY spectrum. Nevertheless, in two larger helical regions several residues (Asp^{48}, Cys^{49}, Tyr^{51} and Lys^{83}, Gln^{84}, Ile^{85}) have similar nitrogen and NH proton chemical shifts, eliminating the possibility of observing an NOE with either experiment.

The assignments of main-chain and side-chain atoms in App-D49 are provided in Table 2. Following the analysis of all spectra, we were unable to identify resonances associated with Tyr^{27} or Cys^{28}. In addition, residues 26, 29 and 30 gave weak cross peaks in many of the spectra. This suggests that the region of the protein between residues 26 and 30 may be disordered.

Assignment of side-chain nuclei

For glycine, serine and other AMX-type spin systems, complete resonance assignments were obtained during assignment of the main-chain atoms. Long aliphatic side-chain ^{1}H and ^{13}C shifts were obtained from the three-dimensional HCCH-TOCSY spectrum. The known assignments of H^{α}, H^{β}, C^{α} and C^{β} atoms were used to extend the assignment through TOCSY transfer to other long-chain proton nuclei. Most of the 15 lysine residues in App-D49 were clustered in a narrow range of carbon and proton frequencies and therefore difficult to assign. However, some of the lysines had nondegenerate chemical shifts for the side-chain protons (e.g. Lys^{110}), indicating that they are located in an anisotropic environment. All observed aliphatic ^{1}H and ^{13}C chemical shifts are within the range of observed chemical shifts reported for other proteins (Grzesiek and Bax, 1992a).

Arginine side-chain amide H^{ε} protons were readily identifiable in the HSQC spectrum and were assigned on the basis of NOEs. Arginine H^{η} and lysine H^{ζ} amide side-chain protons were mostly unresolved. Glutamine and asparagine side-chain amide protons are found in the same region as the backbone amide groups in the ^{15}N-HSQC spectrum. These were identified as having two cross peaks at the same nitrogen shift and adjacent weaker peaks due to deuterium isotope effects from partial deuteration of the side-chain amine proton. Sequence-

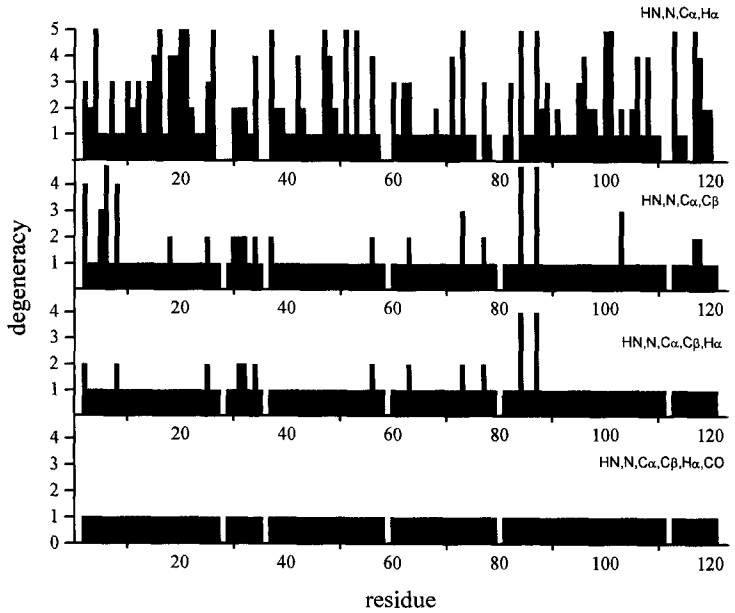

Fig. 3. Degeneracy of resonance assignments. The degeneracy at each residue is shown for interresidue correlations, utilizing the following atoms: HN, N, C^{α}, H^{α} (top), HN, N, C^{α}, C^{β} (second from top), HN, N, C^{α}, C^{β}, H^{α} (second from bottom), and HN, N, C^{α}, C^{β}, H^{α}, CO (bottom). The degeneracy is defined as the number of residues with the same (within experimental error) chemical shifts for the indicated atoms. A degeneracy of 1 implies that the set of chemical shifts is unique, and therefore the residue has been uniquely assigned.

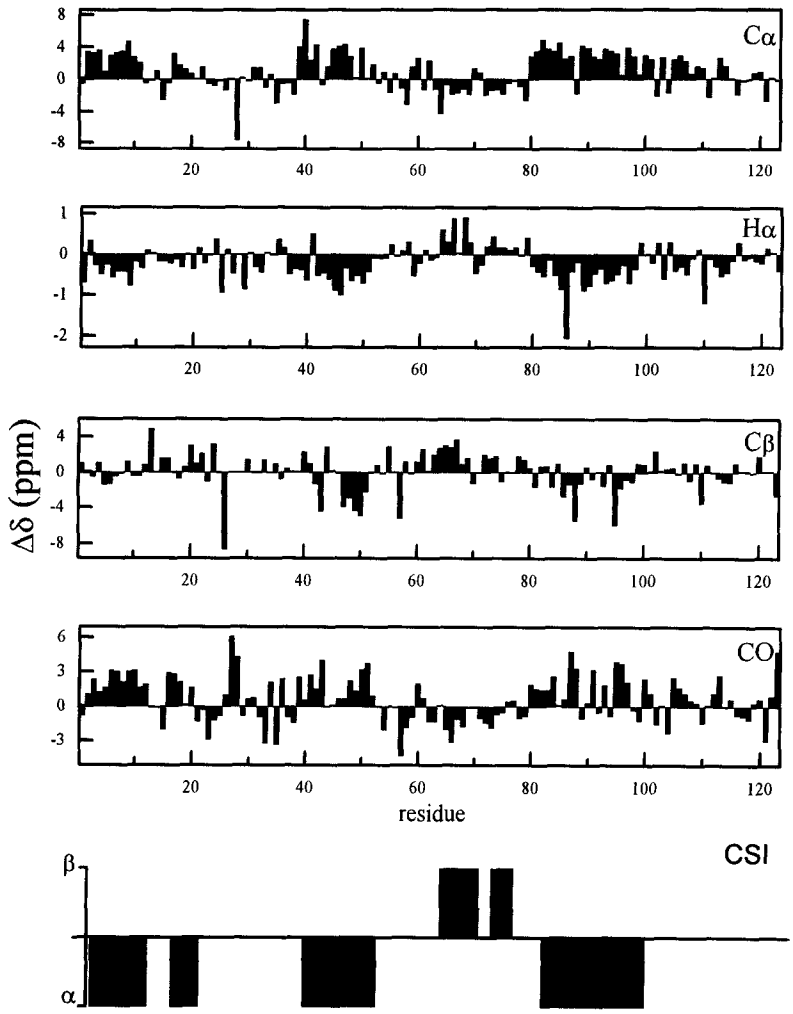

Fig. 4. Chemical shift deviations and chemical shift indexes. The deviation in chemical shifts for the indicated atoms in each residue are shown (C^{α}, H^{α}, C^{β}, CO) in the top four panels. The bottom panel shows the chemical shift index for each residue.

specific assignment of these amides was achieved using the intraresidue NOEs to the side-chain aliphatic protons.

Proton chemical shifts of aromatic side chains were determined from 2D COSY and TOCSY experiments obtained in D_2O. Assignments of the aromatic rings to specific residues were largely made on the basis of a 2D NOESY spectrum obtained in D_2O. Only a limited number of assignments of aromatic residues could be obtained from the CB(CGCD)HD and CB(CGCDCE)HE spectra, due to the low signal-to-noise ratio. The assignment of a large number of aromatic protons was prevented by the degeneracies of the aromatic proton and C^{β} shifts. The three tryptophan H^{ε} resonances were observed in the ^{15}N-HSQC spectrum as well as in the ^{15}N-NOESY-HSQC and ^{15}N-TOCSY-HSQC spectra. Their assignments were obtained from the ^{15}N-NOESY-HSQC spectrum.

Secondary structure of App-D49

It has been shown that the deviation of chemical shifts from random coil values, particularly for C^{α}, C^{β}, CO and H^{α} atoms, depends on the type of secondary structure (Dalgarno et al., 1983). α-Helices cause a positive deviation for C^{α} and CO resonances and a negative deviation for H^{α} and C^{β} resonances. In contrast, β-sheet is characterized by deviations in the opposite sense. The CSI method (Chemical Shift Index; Wishart and Sykes, 1994) combines these deviations to predict secondary structure. In Fig. 4, the deviations of C^{α}, C^{β}, CO and H^{α} shifts from random coil are shown for each residue, together with the chemical shift indexes that were obtained from these deviations. The secondary structure predicted from the chemical shifts is in good agreement with the X-ray structure of the homologous group II PLA2 from human synovial PLA2 (Scott et al., 1991). Three long α-helical segments are clearly distinguishable (residues 2–11, 39–49 and 81–98), as well as the short one-turn helix between residues 17 and 21. A β-sheet, which is composed of two antiparallel β-strands, is positioned at the expected position of residues 63–79. This sheet includes the predicted coil conformation for the β-turn at residues 70 and 71.

Secondary structure information was also obtained

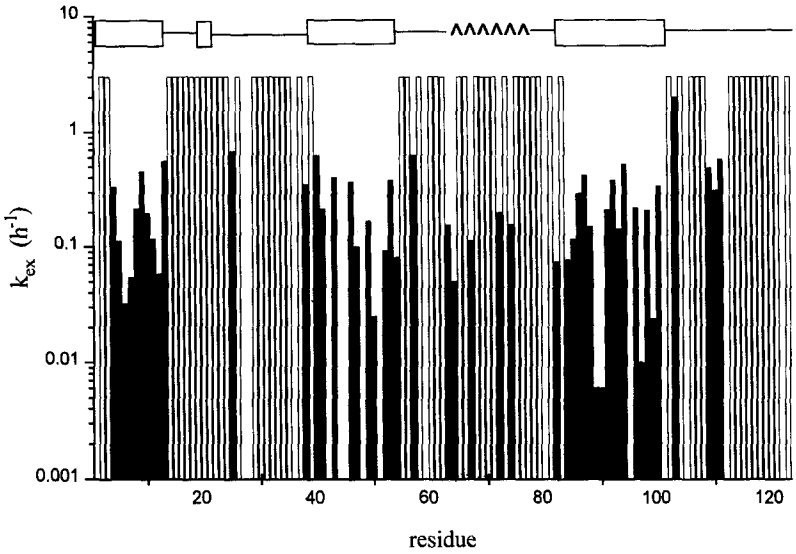

Fig. 5. Amide exchange kinetics. The rate of amide exchange is shown for each residue. A white bar indicates that the rate was too fast to measure. The upper part of the figure schematically shows the secondary structure of App-D49 (□ = helix, ΛΛ = sheet).

from amide hydrogen exchange kinetics (see Fig. 5). Amide protons with slow exchange rates were clustered in three larger regions: residues 4 to 14, 38 to 54 and 82 to 100. These regions map to the three longer helices in all known group I and II PLA2s. Amide protons in the region of residues 82–100 (third long helix) were the most protected from exchange. Twelve of the protons from this region (86–97) were still observable after two months of exchange. In contrast, only residues 8 and 9 in the first helix and residues 42, 48 (active-site histidine) and 49 from the third helix were visible after this period. No protection from exchange was observed in the region 18–21, which corresponds to the one-turn helix in crystal structures; this suggests that the H-bonds in this helix are less protected or that the helix is less stable in solution. In the region corresponding to the β-sheet, exchange of the amides from residues 67, 72 and 74 was observed. However, the last residue overlaps with the amide of Lys^{83}, making an unambiguous assignment difficult. Particularly noticeable is the protection of the surface loop Trp^{109}-Tyr^{111}, suggesting that this region of App-D49 may form a loop with fairly stable hydrogen bonds.

Additional information on the secondary structure of residues was obtained by measurement of the coupling between the HN and H^{α} protons. α-Helical regions are characterized by coupling constants of less than approximately 5 Hz. β-Strands possess coupling constants larger than 8 Hz. The $J_{H^N\text{-}H^{\alpha}}$ coupling constants for all residues are shown schematically in Fig. 6. The measured coupling constants are in agreement with other indicators of secondary structure type. Coupling constants are less than 5 Hz for amino-terminal residues up to Lys^{11} (except for Gln^4: 5.7 Hz). In particular, the coupling constants were 4.0 and 2.5 Hz for Leu^2 and Phe^3, respectively. For most of the residues in the central helix (residues 82 to 99), the coupling constants were less than 5 Hz. The short, one-turn helix (residues 17–21) displays coupling constants that are greater than what would be expected for an α-helix, suggesting that this helix is either distorted or somewhat unstable. The second long helix (residues 40–54) contains some residues whose coupling constants are greater than 5 Hz, suggesting that this helix may be distorted. The β-sheet region, residues 61 through 79, shows moderate to large coupling constants (with the exception of the β-turn), which indicates that this region is in a well-defined extended conformation.

Finally, secondary structure elements in App-D49 were also characterized by a specific pattern of sequential and long-range NOE cross peaks (Wüthrich, 1986). An example of a section of the ^{15}N-NOESY-HMQC spectrum, which shows NOEs to residues 2 and 5, is shown in Fig. 7. Interresidual NOE data for each residue in App-D49 are schematically displayed in Fig. 6. The first helix (1–13) is defined by strong HN-HN and $H^{\beta}N$ NOEs. A number of long-range connections (i,i+3; i,i+4) are present between H^{α} and NH protons in the helical regions, particularly the amino-terminal helix. The second helix (residues 40–50) is less defined, due to the overlap in NH and N chemical shifts, but is characterized by several strong i,i+4 and i,i+3 NOEs. The third helix (residues 80–100) can be recognized from strong NH-NH, H^{β}-NH, and H^{α}-NH(i,i+3) NOEs. The two-stranded β-sheet is defined by strong sequential H^{α}-NH NOEs as well as long-range interstrand NOEs (see Fig. 8). The long-range NOEs in the β-sheet allow identification of hydrogen-bonding partners. The HN-HN NOEs between residues 70–72 are characteristic of a type I turn (Wüthrich, 1986). The hydrogen-bonding pattern and type of turn make this entire segment of the protein essentially identical to the same β-sheet in the pancreatic enzyme.

Discussion

The secondary structure of App-D49 shows some similarities to the pancreatic enzyme in solution. In the case of App-D49, the calcium-binding loop of the free enzyme also appears to be flexible, thus offering an explanation for the absence of resonances of residues Tyr^{27} and Cys^{28} and the weak intensity of Gly^{29}, Trp^{30} and Cys^{26} in our data. The addition of Ca^{2+} to the pancreatic enzyme appears to stabilize the calcium-binding loop (Van den Berg et al., 1995a,b), and it is likely that a similar effect would be observed in App-D49. In addition to the calcium-binding loop, a number of secondary structure elements in App-D49 are similar to those present in the pancreatic enzyme. In particular, the long-range NOEs across the β-sheet indicate that this structure is similar in both enzymes. Additionally, the second and third helices appear to be similar in both proteins as well.

These similarities aside, there are also a number of significant differences between the secondary structures of App-D49 and the pancreatic enzyme in solution. NMR studies on the group I enzyme from pancreas have identified a number of conformational changes in the protein structure that occur as a result of formation of the complex of protein, Ca^{2+}, lipid, and inhibitor (Van den Berg et al., 1995a,b). In particular, formation of the complex resulted in stabilization of the amino-terminal helix and residues 69 through 72. In the ternary complex, but not in the free enzyme in solution, the position of the amino terminus is fixed by hydrogen bonds to the side chain of Gln^4 and to the main chain of residues 69 and 71. A well-defined conformation of these residues is thought to be important for generation of a catalytically important hydrogen-bonded network, involving His^{48}, Asp^{99}, Tyr^{73}, Tyr^{52} and the amino terminus.

There seems to be a distinct difference between the structure of the pancreatic enzyme in solution or in a crystalline environment. However, crystallographic studies suggest that few structural changes occur due to formation of the protein–inhibitor complex for either group I or group II enzymes. For example, in the crystal structure of the human nonpancreatic secretory enzyme (group II) in complex with an inhibitor (Scott et al., 1991), the amino-terminal region of the protein is well defined. The amino-terminal helix is present, the residues involved in the hydrogen-bond network are ordered, and residues responsible for fixing the position of the amino terminus are also ordered. Therefore, the possibility must be considered that in the group II enzymes, lipid-induced conformational changes of the amino terminus and residues 69–72 may not play a significant role in interfacial activation.

On the basis of the data presented here, the amino-terminal helix of App-D49 appears to be well defined in solution. We have observed distinct HN-HN cross peaks in the entire region of residues 1–14. Furthermore, short-range NOEs are observed between H^{α} of Leu^2 and the HN proton of Phe^5. Additional long-range NOEs are seen

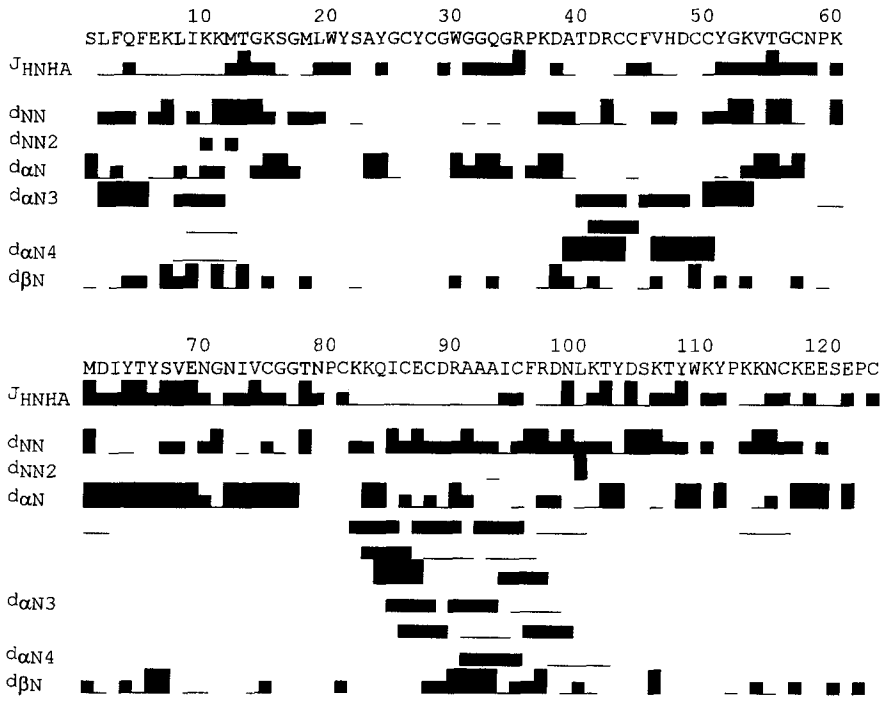

Fig. 6. $J_{H^N\text{-}H^\alpha}$ coupling constants and NOEs for all residues in App-D49. The absence of a symbol indicates that it was not possible to measure the coupling constant, due to overlap in the HNHA spectrum. NOEs between HN protons on adjacent residues are indicated as d_{NN}. NOEs between HN protons of residues i and i+2 are indicated by d_{NN2}. Sequential NOEs between H^α protons and the i, i+3, and i+4 HN protons are indicated as $d_{\alpha N}$, $d_{\alpha N3}$ and $d_{\alpha N4}$, respectively. NOEs between H^β and the HN of the following residue are indicated as $d_{\beta N}$.

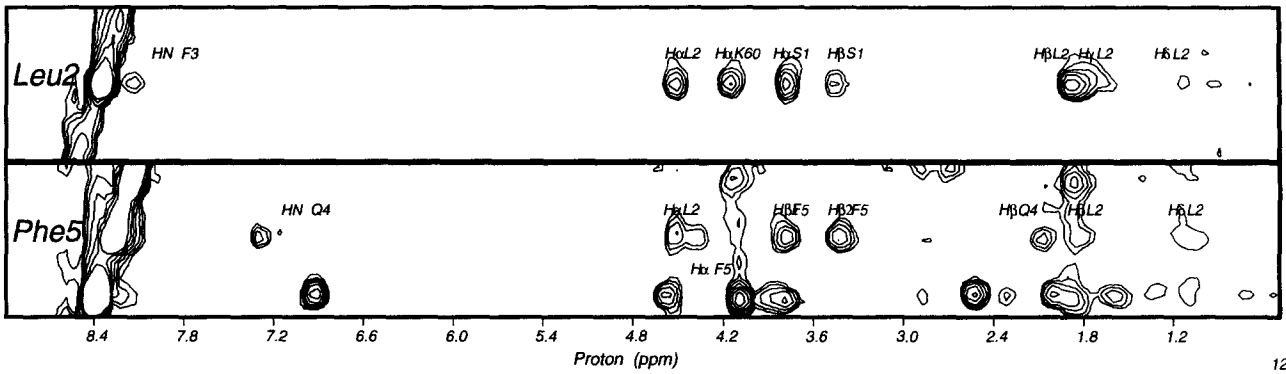

Fig. 7. Portions of the NOESY ^{15}N-HSQC spectrum, containing the amide protons of Leu^2 (top) and Phe^5 (bottom). The assigned cross peaks are identified with the names of the protons that are dipolarly coupled to the amide proton.

between the HN proton of Leu^2 and the H$^\alpha$ proton of Lys^{60} (see Fig. 7) and the side-chain protons of Gln^4 and the H$^\alpha$ proton of Tyr^{64} (not shown). Further supporting evidence for a helical conformation of the amino-terminal region are the deviations from random coil chemical shifts. Chemical shifts of C$^\alpha$ resonances deviate from the random coil values by 3.6, 3.4 and 3.8 ppm for Leu^2, Phe^3 and Gln^4, respectively. This suggests that these residues are in a helical conformation. Additionally, the $J_{H^N\text{-}H^\alpha}$ coupling constants of the amino-terminal residues are less than 5 Hz, which is characteristic of an α-helical conformation. Finally, the amide protons of residues Gln^4 through Thr^{13} are protected from exchange, indicating stable hydrogen bonds to the carbonyls of residues 1 through 9. The rates of amide exchange for these residues (0.1 h^{-1}) are considerably less than found for the pancreatic enzyme in solution (Peters et al., 1992).

We have tentatively identified the resonance line of the terminal amino group. In the ^{15}N-HSQC spectrum, we have observed a cross peak at a nitrogen chemical shift of approximately 32 ppm, which is characteristic of the terminal amino group (Fig. 1). Under the experimental conditions employed in this study, it would be difficult to observe this resonance unless it were protected from solvent. We also found three additional cross peaks at a similar nitrogen chemical shift, which we were unable to assign. These peaks probably arise from the side-chain amides of lysine residues. Cross peaks at similar chemical shifts appeared in the NMR spectrum of the pancreatic PLA2 upon its binding to the micelles and inhibitor, and one of them was tentatively assigned to the H$^\zeta$ proton of Lys^{56}.

The position of the amino terminus may also be fixed by interactions with amino acids in the region of residue Ile^{63}. This region is close to the elapid loop, which is present in the pancreatic enzyme, but absent in group II lipases. There is evidence that these residues in App-D49 are ordered in solution and are involved in docking of the amino terminus. All of the $J_{H^N\text{-}H^\alpha}$ coupling constants for this region are larger than what would be expected, due to conformational averaging. Additionally, we observe strong H$^\alpha$-NH NOEs and weak HN-HN NOEs. Furthermore, residues 63 and 64 are protected from amide exchange, indicating that these residues are involved in stable hydrogen bonds. Finally, there are several intense NOEs from this region to the amino-terminal residues.

On the basis of the data presented here, we conclude

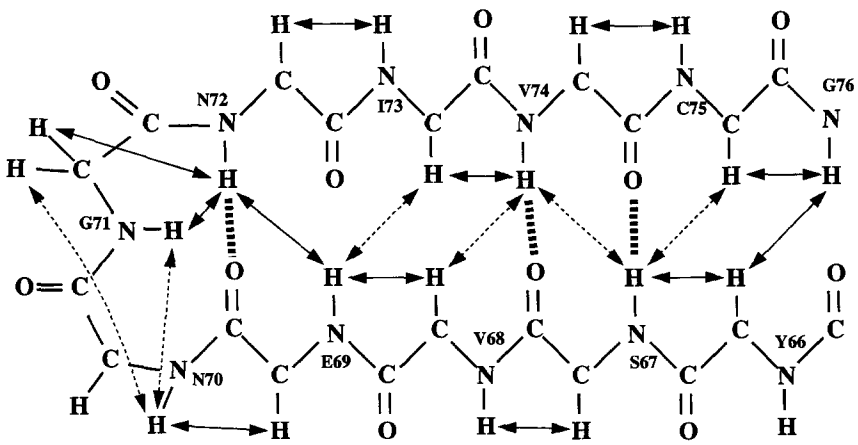

Fig. 8. NOE interactions in the β-sheet of App-D49. NOEs between residues Gly^{76} through Tyr^{66} are indicated. Solid arrows represent relatively intense NOEs, dotted arrows represent weaker NOEs. The dashed lines indicate hydrogen bonds that were inferred from the kinetics of amide exchange.

that in this representative of group II phospholipases the amino-terminal helix is completely formed in solution and is already positioned in such a manner as to be effective for catalysis. This observation is supported by chemical modification studies by Verheij et al. (1981), which showed that efficient modification of the amino terminus of type II phospholipases only occurs when the proteins are partially denatured.

The difference in the conformation of the amino-terminal helix in group I and group II enzymes is not likely to be due to the differences in position of disulfide bonds. In group I PLA2s, the amino-terminal helix is configurationally restricted due to the presence of a disulfide bond (at residue 11) to the β-sheet, while this constraint is absent in all group II PLA2s. This difference in covalent structure would be expected to confer additional stability to the amino-terminal residues of group I enzymes, yet the opposite is observed in the case of the pancreatic enzyme. Therefore, the instability of the amino terminus in the pancreatic enzyme is likely a reflection of somewhat weaker noncovalent interactions in this region of the protein compared to those seen in App-D49. Deletion of the elapid loop (residues 62–66) of the pancreatic PLA resulted in increased activity towards micelles and a reduction in the mobility of this region (Kuipers et al., 1989). Therefore, the elapid loop may be responsible for the reduced stability of the amino-terminal helix in the group I enzymes. Since the amino-terminal helix exists in App-D49, and is likely marginally stable in the pancreatic enzyme, we conclude that formation of this helix is a necessary, but not sufficient, step in activation of phospholipases.

The importance of the amino-terminal group for enzymatic activity towards aggregated substrates is well known from biochemical data. Phospholipases with a chemically modified amino group, or with an amino-terminal extension, lose their ability for interfacial activation (Verheij et al., 1981). It has been postulated that the amino terminus participates in the formation of a hydrogen-bonding network that extends to the active site. However, the actual role of the amino terminus in catalysis has not been fully defined. Studies by Tsai and coworkers (Dupureur et al., 1992) strongly suggest that the hydrogen-bonding network has only a minor contribution to catalysis. Therefore, other properties of the amino terminus, such as net positive charge (Scott and Sigler, 1994), may be important for activity.

Conclusions

In summary, we have reported the almost complete assignment of ^{1}H, ^{15}N and ^{13}C resonances of PLA2 from *Agkistrodon piscivorus piscivorus*. The secondary structure is consistent with X-ray structures for homologous group II phospholipases. NOE data, coupling constants, chemical shift values and hydrogen exchange experiments indicate that the first amino-terminal helix is well defined in solution. This is in contrast to the group I pancreatic phospholipase, where the first three residues become ordered upon binding to the micelles in the presence of a transition-state analog. These structural differences are likely due to minor differences in the stability of the amino-terminal helix in both enzymes and may not reflect intrinsic differences in the mechanism of activation of group I and group II enzymes.

Acknowledgements

We thank Dr. Brian Lathrop for help in the purification of the ^{15}N-labeled App-D49. This research was supported by a grant from the NSF (DMB9305002) to G.S.R. and R.L.B. and by a grant from the NIH (GM37658) to R.L.B. The NMR spectrometer was purchased, in part, by a shared equipment grant from the NSF (BIR-9217013). R.J. was supported in part by the Ministry of Science and Technology of Slovenia.

References

Almeida, P.F., Jerala, R., Rule, G.S. and Biltonen, R.L. (1995) *Biophys. J.*, **68**, A184.

Archer, S.J., Ikura, M., Torchia, D.A. and Bax, A. (1991) *J. Magn. Reson.*, **95**, 636–641.

Bax, A., Ikura, M., Kay, L.E., Torchia, D.A. and Tschudin, R. (1990a) *J. Magn. Reson.*, **36**, 304–318.

Bax, A., Clore, M. and Gronenborn, A.M. (1990b) *J. Magn. Reson.*, **88**, 425–431.

Bax, A. and Pochapsky, S. (1992) *J. Magn. Reson.*, **99**, 638–643.

Bax, A., Vuister, G.W., Grzesiek, S., Delaglio, F., Wang, A.C., Tschudin, R. and Zhu, G. (1994) *Methods Enzymol.*, **239**, 79–105.

Bell, J.D. and Biltonen, R.L. (1989) *J. Biol. Chem.*, **264**, 12194–12200.

Bell, J.D. and Biltonen, R.L. (1992) *J. Biol. Chem.*, **267**, 11046–11056.

Billeter, M., Braun, W. and Wüthrich, K. (1982) *J. Mol. Biol.*, **155**, 321–346.

Biltonen, R.L., Lathrop, B.K. and Bell, J.D. (1991) *Methods Enzymol.*, **197**, 234–248.

Bodenhausen, G. and Ruben, D.G. (1980) *Chem. Phys. Lett.*, **69**, 185–189.

Burack, W.R., Yuan, Q. and Biltonen, R.L. (1993) *Biochemistry*, **32**, 583–589.

Burgoyne, R.D. and Morgan, A. (1990) *Trends Biochem. Sci.*, **15**, 365–366.

Cho, W., Tomaselli, A.G., Heinrikson, R.L. and Kezdy, F.J. (1988) *J. Biol. Chem.*, **263**, 11237–11241.

Clubb, R.T., Thanabal, V. and Wagner, G. (1992) *J. Biomol. NMR*, **2**, 203–210.

Dalgarno, D.C., Levine, A. and Williams, R.J.P. (1983) *Biosci. Rep.*, **3**, 443–452.

Dennis, E.A. (1987) *Biotechnology*, **5**, 1294–1300.

Driscoll, P.C., Clore, G.M., Marion, D., Wingfield, P.T. and Gronenborn, A.M. (1990) *Biochemistry*, **29**, 3542–3556.

Dupureur, C.M., Yu, B.-Z., Jain, M.K., Noel, J.P., Deng, T., Li, Y., Byeon, I.-J.L. and Tsai, M.-D. (1992) *Biochemistry*, **32**, 6402–6413.

Edison, A.S., Abilgaard, F., Westler, W.M., Mooberry, S. and Markley, J.L. (1994) *Methods Enzymol.*, **239**, 3–79.

Frenkiel, T., Bauer, C., Carr, M.D., Birdsall, B. and Feeney, J. (1990) *J. Magn. Reson.*, **90**, 420–425.

Grzesiek, S. and Bax, A. (1992a) *J. Magn. Reson.*, **96**, 432–440.

Grzesiek, S. and Bax, A. (1992b) *J. Am. Chem. Soc.*, **114**, 6291–6293.

Grzesiek, S. and Bax, A. (1993) *J. Biomol. NMR*, **3**, 185–204.

Heinrikson, R.L., Krueger, E.T. and Keim, P.S. (1977) *J. Biol. Chem.*, **252**, 4913–4921.

Ikura, M., Bax, A., Clore, G.M. and Gronenborn, A.M. (1990) *J. Am. Chem. Soc.*, **112**, 9020–9022.

Jain, M.K. and Maliwal, B.P. (1993) *Biochemistry*, **32**, 11838–11846.

Jerala, R. and Rule, G.S. (1995) *J. Magn. Reson. Ser. B*, **108**, 294–298.

Kay, L.E., Ikura, M., Tschudin, R. and Bax, A. (1990) *J. Magn. Reson.*, **89**, 496–514.

Kuipers, O.P., Thunnissen, M.M.G.M., De Geus, P., Dijkstra, B.W., Drenth, J., Verheij, H.M. and De Haas, G.H. (1989) *Science*, **244**, 82–85.

Lathrop, B.K., Burack, W.R., Biltonen, R.L. and Rule, G.S. (1992) *Protein Exp. Purif.*, **3**, 512–517.

Lichtenberg, D., Romero, G., Menashe, M. and Biltonen, R.L. (1986) *J. Biol. Chem.*, **261**, 5334–5340.

Maragonore, J.M. and Heinrikson, R.L. (1993) *J. Biol. Chem.*, **268**, 6064.

Marion, D., Ikura, M., Tschudin, R. and Bax, A. (1989a) *J. Magn. Reson.*, **85**, 393–399.

Marion, D., Ikura, M. and Bax, A. (1989b) *J. Magn. Reson.*, **85**, 425–430.

Menashe, M., Romero, G., Biltonen, R.L. and Lichtenberg, D. (1986) *J. Biol. Chem.*, **261**, 5328–5333.

Messerle, B.A., Wider, G., Otting, G., Weber, C. and Wüthrich, K. (1989) *J. Magn. Reson.*, **85**, 608–613.

Olejniczak, E.T. and Eaton, H. (1990) *J. Magn. Reson.*, **87**, 628–632.

Peters, A.P., Dekker, N., Van den Berg, L., Boelens, R., Kaptein, R., Slotboom, A.J. and De Haas, G. (1992) *Biochemistry*, **31**, 10024–10030.

Renetseder, R., Brunie, S., Dijkstra, B.W., Drenth, J. and Sigler, P. (1985) *J. Biol. Chem.*, **260**, 11627–11634.

Scott, D.L., White, S.P., Otwinowski, Z., Yuan, W., Gelb, M.H. and Sigler, P.B. (1990) *Science*, **250**, 1541–1546.

Scott, D.L., White, S.P., Browning, J.L., Rosa, J.J., Gelb, M.H. and Sigler, P.B. (1991) *Science*, **254**, 1007–1010.

Scott, D.L. and Sigler, P.B. (1994) *Adv. Protein Chem.*, **45**, 53–88.

Slotboom, A.J., Verheij, H.M. and De Haas, G.D. (1982) In *Phospholipids* (Eds, Hawthorne, J.N. and Ansell, G.B.), Elsevier Press, Amsterdam, The Netherlands.

Van Dam-Mieras, M.C., Slotboom, A.J., Pieterson, W.A. and De Haas, G.H. (1975) *Biochemistry*, **14**, 5387–5394.

Van den Berg, B., Tessari, M., Boelens, R., Dijkman, R., Kaptein, R. and De Haas, G. (1995a) *J. Biomol. NMR*, **5**, 110–121.

Van den Berg, B., Tessari, M., Boelens, R., Dijkman, R., De Haas, G., Kaptein, R. and Verheij, H.M. (1995b) *Nature Struct. Biol.*, **2**, 402–406.

Verheij, H.M., Egmond, M.R. and De Haas, G.H. (1981) *Biochemistry*, **20**, 94–99.

Vuister, G.W. and Bax, A. (1993) *J. Am. Chem. Soc.*, **115**, 7772–7777.

Wang, A.C., Lodi, P.J., Qin, J., Vuister, G.W., Gronenborn, A.M. and Clore, G.M. (1994) *J. Magn. Reson. Ser. B*, **105**, 196–198.

Wishart, D.S. and Sykes, B.D. (1994) *Methods Enzymol.*, **239**, 363–392.

Wittekind, W. and Mueller, L. (1993) *J. Magn. Reson. Ser. B*, **101**, 201–205.

Wüthrich, K. (1986) *NMR of Proteins and Nucleic Acids*, Wiley, New York, NY.

Yamazaki, T., Forman-Kay, J.D. and Kay, L.E. (1993) *J. Am. Chem. Soc.*, **115**, 11054–11055.